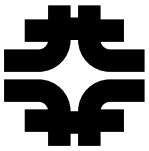

# Fermi National Accelerator Laboratory

**FERMILAB-Pub-99/018**

# Edgeworth Series for Collision Energy Loss and Multiple Scattering

A. VanGinneken

*Fermi National Accelerator Laboratory*
*P.O. Box 500, Batavia, Illinois 60510*

February 1999

Submitted to *Nuclear Instruments and Methods A*

Operated by Universities Research Association Inc. under Contract No. DE-AC02-76CH03000 with the United States Department of Energy

# Edgeworth Series for Collision Energy Loss and Multiple Scattering

A. Van Ginneken *
Fermi National Accelerator Laboratory†
P. O. Box 500, Batavia, IL 60510

February 11, 1999

**Abstract**

The Edgeworth expansion is used to go beyond the usual Gaussian approximation for collision energy loss and multiple scattering. Monte Carlo algorithms based on the expansion are presented. Comparisons of the Edgeworth expansion with exact results of Vavilov and Moliere are shown. A simple model which attempts to include correlations between energy loss and angular distribution is proposed and illustrated with an example.

## 1 Introduction

This note investigates the Edgeworth expansion of the Gaussian approximation for collision energy loss and multiple scattering of charged particles along with their implementation into Monte Carlo subroutines. The main motivation is the demand for realistic simulations of muon ionization cooling [1]. This note therefore deals with muon projectiles although practically all of it readily translates to other charged particles. In an ionization cooling channel a muon beam cools by repeatedly traversing absorbers and re-accelerating cavities with net loss of transverse momentum. The muons also undergo multiple scattering in the absorbers which heats the beam. In the entire process a muon can lose and regain many times its original energy making the need for realistic simulations obvious. Particular attention must

*Tel.: +1 (630) 840 3464; e-mail: vangin@fnal.gov

†Fermi National Accelerator Laboratory is operated by Universities Research Association under contract No. DE-AC02-76CH03000 with the US Department of Energy.

be paid to the tails of both energy loss and angular distributions. Muons which undergo a large deflection or energy loss have a high probability of being lost from the beam. Another concern is that of correlations between energy loss and angle which may have similar undesirable consequences. Such correlations are introduced when muons interact with atomic electrons which get ejected from the atom, a process that accounts for a significant portion of the muon's total energy loss and is approximated as free $\mu e^-$ scattering in which energy loss and scattering angle are fully correlated. Since the mean square angle for scattering off all atomic electrons is proportional to $Z$ while for scattering off the nucleus it goes as $Z^2$, one expects the overall correlation with energy loss to be stronger for low-$Z$ materials. Because of smaller multiple scattering angles, low-$Z$ materials are also more effective for ionization cooling, which makes the correlations more worrisome in this application. By contrast, excitation of the atom—where an electron is promoted to a higher orbit—results in atomic recoil which takes relatively little of the energy lost by the muon and thus introduces very little correlation. Below, a simple model is proposed which separates these processes and which exploits the newly minted algorithms based on the Edgeworth series.

For thick enough targets both energy loss and (projected) multiple scattering distributions are well represented by a Gaussian. However, such thicknesses are too large to serve as a typical step in a Monte Carlo—particularly for ionization cooling. When a cut-off energy or angle is introduced—which leaves events with large angle scattering and energy loss to be treated individually [2]—the Gaussian approximation gains in validity when it is used to represent, collectively, all events below such a threshold. The number of events to be simulated individually increases inversely with the restriction threshold adopted. The strategy for energy loss in [3], e.g., is to simulate some 10 individual events per step and add a random Gaussian energy loss to account for the rest. This is no doubt fine for many applications but should probably be refined for ionization cooling—particularly in the tails. The gist of the present method is to replace the Gaussian with the Edgeworth expansion [4] which is capable of representing the non-Gaussian tails quite accurately. Most importantly, the Edgeworth series provides a framework which allows new or improved physical models to be easily translated into algorithms. The coefficients of the series relate directly to the moments of the single scattering or energy loss law. A new or refined model will produce more accurate estimates of the moments which then produces a more accurate algorithm. For thinner targets the deviations from a Gaussian are larger and higher order terms of the series become more important.

In sec. 2 what is needed about the Edgeworth expansion and how it relates to the present problem is briefly stated. A simple model is proposed in sec. 3 which aims at providing a first order approximation to study correlations between energy loss and angle after traversing a target. Implementation of this model and of the Edgeworth series into Monte Carlo algorithms is indicated in sec. 4. Sec. 5 contains a few results obtained with this method including comparisons with analytic results of Vavilov and Molière. Concluding remarks are in sec. 6. In some ways, this note is a continuation of [2].

## 2 Edgeworth Expansion

The Edgeworth series is a well known method [4] to introduce corrections to a Gaussian distribution, $G(x)$,

$$\begin{aligned} F(x) \quad = G(x) \, [ \quad & 1 \\ & + \frac{\kappa_3}{3! \kappa_2^{\frac{3}{2}}} H_3(x) \\ & + \frac{\kappa_4}{4! \kappa_2^2} H_4(x) + \frac{10 \kappa_3^2}{6! \kappa_2^3} H_6(x) \\ & + \frac{\kappa_5}{5! \kappa_2^{\frac{5}{2}}} H_5(x) + \frac{35 \kappa_3 \kappa_4}{7! \kappa_2^{\frac{7}{2}}} H_7(x) + \frac{280 \kappa_3^3}{9! \kappa_2^{\frac{9}{2}}} H_9(x) \\ & + \ldots \, ] \end{aligned} \tag{1}$$

where the $H_i$ are Hermite polynomials and $\kappa_i$ are the cumulants of distribution $F(x)$. Note that the denominators appear exclusively as powers of $\kappa_2 (= \sigma^2)$, the variance of $F(x)$. The terms on each line of eq.(1) are of the same order of approximation, where order here can be equated with inverse power of $\kappa^{1/2}$ with, e.g, the last line written out in (1) being of third order. It is important when either continuing or abbreviating eq.(1) to do so by one or more full orders [4, 5]. The number of terms grows linearly with order. Likewise the $H_i(x)$ grow in number of terms with $i$ and the coefficients of the $x^n$ belonging to each $H_i(x)$ grow quickly in magnitude with $i$. These combined growth processes limit the order to which one may reasonably aspire, even with the aid of a computer. For both energy loss and multiple scattering the $\kappa_i$ are relatively easily obtained—an obvious necessity for the method to succeed. The Landau-Vavilov [6, 7] derivation of the energy loss

distribution starts from the differential equation:

$$\frac{\partial F(t,\Delta E)}{\partial t} = \int_0^{(\Delta E,\epsilon_c)_{min}} \omega(\epsilon) F(t,\Delta E-\epsilon)\, d\epsilon - F(t,\Delta E)\int_0^{\epsilon_c} \omega(\epsilon)\, d\epsilon \quad (2)$$

where $\Delta E = E_0 - E$ is the energy loss over pathlength $t$ of a particle, $\omega(\epsilon)$ is the probability to lose energy, $\epsilon$, per unit length in an infinitesimally thin target, and $\epsilon_c$ is either the maximum energy loss in a single collision, $\epsilon_{max}$, or it may represent a restriction threshold above which collisions are to be simulated as individual events. From eq.(2) Vavilov [7] obtains the Laplace transform of $F(t,\Delta E)$

$$\rho(t,p) = e^{-t\int_0^{\epsilon_c}\omega(\epsilon)(1-e^{-\epsilon p})\,d\epsilon}. \quad (3)$$

Alas, for the $\omega(\epsilon)$ of interest here, the inverse transform of $\rho(t,p)$ is not so simple.

Recall that, in probability language, the Laplace transform, $\rho(t,p)$, is the *moment generating* function of $F(t,\Delta)$ and that $\ln\rho(t,p)$ is its *cumulant generating* function which, in the present case, may be expressed as

$$\ln\rho(t,p) = -t\int_0^{\epsilon_c}\omega(\epsilon)\left(1-e^{-\epsilon p}\right)\,d\epsilon = \kappa_1 p - \kappa_2\frac{p^2}{2!} + \kappa_3\frac{p^3}{3!} - \ldots\ . \quad (4)$$

Expanding the exponential under the integral sign of eq.(4) permits the identifications

$$\kappa_i = t\int_0^{\epsilon_c}\epsilon^i\omega(\epsilon)\,d\epsilon, \quad (5)$$

i.e., for all $i$ the cumulants are essentially the moments of $\omega(\epsilon)$. Note that no special restrictions are placed on $\omega(\epsilon)$. For the present purpose the $\omega(\epsilon)$ of most interest is Bhabha's formula describing $J = 1/2$ particles scattering off electrons [8]

$$\omega(\epsilon) = \frac{\xi}{\epsilon^2}\left[1 - \beta^2\frac{\epsilon}{\epsilon_{max}} + \frac{\epsilon^2}{2E_0^2}\right] \quad (6)$$

where $\xi = 2\pi N_{Av} Z r_e^2 m_e/(A\beta^2)$ and $N_{Av}$ denotes Avogadro's number, $m_e$ the electron mass, $r_e$ its classical radius, $Z$ and $A$ the charge and mass number of the atom, and $\beta$ the velocity in units of the speed of light. In eq.(6) $\omega(\epsilon)$ expresses the energy loss distribution for an infinitesimal target per unit 'length' expressed as unit mass per unit area. For $J = 0$ particles (instead of muons) scattering off electrons the last term in the bracket of eq.(6) is absent. In the Landau approximation the middle term is also

absent. For all of these, the integrals of eq.(5) are easily carried out and result in simple algebraic expressions.

For multiple scattering, a differential equation quite similar to eq.(2) may be written with $\epsilon$ replaced by the *projected* scattering angle

$$\frac{\partial S(t,\theta_x)}{\partial t} = \int_{-\infty}^{\infty} v(\theta'_x) S(t, \theta_x - \theta'_x)\, d\theta'_x - S(t,\theta_x) \int_{-\infty}^{\infty} v(\theta'_x)\, d\theta'_x \qquad (7)$$

where $v(\theta_x)$ is the probability of scattering through projected angle $\theta_x$ per unit length in an infinitesimally thin target. Eq.(7) is independent of $\theta_y$ which has a distribution obeying the same equation. Since $\theta_x$ ranges over negative as well as positive values one would proceed with the Fourier transform of eq.(7), rather than the Laplace transform as done for eq.(2). An expression similar to eq.(3) is obtained which, in probability language, may be identified as the *characteristic* function of $S(t,\theta_x)$. Its logarithm is likewise called a cumulant generating function, related to but different from eq.(4), which also leads to the same type of expression for the cumulants

$$\kappa'_i = t \int_{-\infty}^{\infty} \theta_x^i v(\theta_x)\, d\theta_x. \qquad (8)$$

Again $v(\theta_x)$ has no special restriction placed on it and $v(\theta_x)$ could vanish beyond some cut-off angle, either dictated by physical condiderations such as finite nuclear size [9] or self-imposed to improve the approximation. Attention here is confined to Rutherford scattering and its variants. Since $v(\theta_x)$ is symmetric about zero the $\kappa'_i$ vanish for odd $i$ and many of the terms of eq.(1) along with it. This improves convergence and allows, with an effort comparable to the energy loss case, to pursue higher orders of approximations.

The Edgeworth series offers considerable convenience for simulations. A different physical model means only that a new set of $\kappa_i$ must be calculated but eq.(1)—and the Monte Carlo algorithm—remain the same otherwise.

# 3 Physical Model

A physical model is proposed here which separates events with electron recoil from those with atomic recoil in order to study correlations between energy loss and angle in ionization cooling.

## 3.1 Energy Loss

For muons colliding with free electrons the scattering law is eq.(6). When $\epsilon$ is large compared with the mean ionization potential, $\epsilon_i$, eq.(6) can be expected

to hold even when the target electron is bound to an atom. When $\epsilon \ll \epsilon_i$ the muon can only excite—not ionize—the atom and one expects a different law to govern such events. The model here makes the simplest possible assumption, viz., collisions with energy transfers *below* $\epsilon_i$ result in atomic recoil. The recoil is neglected and the momentum transfer to the muon—or its angle of deflection—is uncorrelated with energy loss and treated as part of the nuclear scattering. Energy transfers *above* $\epsilon_i$ are assumed to take place with free electrons with full correlation between energy loss and angular deflection.

It remains to decide which energy loss law to adopt below $\epsilon_i$. One could ignore $\epsilon_i$ and assume eq.(6) to apply down to some $\epsilon_{min}$ which is specified by the condition

$$\int_{\epsilon_{min}}^{\epsilon_c} \epsilon\omega(\epsilon)\, d\epsilon = \frac{dE_{restr}}{dx}. \tag{9}$$

This is equivalent to Vavilov's approach (with a restriction threshold [2]). However, $\epsilon_{min}$ thus obtained is very small compared with typical separations between energy levels available to the electron—yet the $\epsilon^{-2}$ law predicts the largest number of collisions near $\epsilon_{min}$. Perhaps the next simplest assumption is

$$\omega_<(\epsilon) = \frac{\xi\epsilon_i}{\epsilon^3} \tag{10}$$

which guarantees a higher $\epsilon_{min}$ while leaving $\omega(\epsilon)$ approximately continuous at $\epsilon_i$. The condition equivalent to eq.(9) now demands that

$$\int_{\epsilon_{min}}^{\epsilon_i} \epsilon\omega_<(\epsilon)\, d\epsilon + \int_{\epsilon_i}^{\epsilon_c} \epsilon\omega_>(\epsilon)\, d\epsilon = \frac{dE_{restr}}{dx}. \tag{11}$$

where $\omega_>(\epsilon)$ is the same as $\omega(\epsilon)$ of eq.(6). The second term of eq.(11) yields

$$\int_{\epsilon_i}^{\epsilon_c} \epsilon\omega_>(\epsilon)\, d\epsilon = \xi\left[\ln(\frac{\epsilon_c}{\epsilon i}) - \beta^2\frac{\epsilon_c - \epsilon_i}{\epsilon_{max}} + \frac{\epsilon_c^2 - \epsilon_i^2}{4E_0^2}\right] \tag{12}$$

which may be compared with the Bethe-Bloch formula for restricted energy loss [10]

$$\frac{dE_{restr}}{dx} = \xi\left[\ln(\frac{2m_e\beta^2\gamma^2\epsilon_c}{\epsilon_i^2}) - \beta^2(1 + \frac{\epsilon_c}{\epsilon_{max}}) - \delta\right] \tag{13}$$

where $\gamma$ is the muon energy in units of its mass, and $\delta$ is the density effect correction [11]. Subtracting eq.(12) from eq.(13):

$$\int_{\epsilon_{min}}^{\epsilon_i} \epsilon\omega_<(\epsilon)\, d\epsilon = \xi\left(\frac{\epsilon_i}{\epsilon_{min}} - 1\right) = \xi\left[\ln(\frac{2m_e\beta^2\gamma^2}{\epsilon_i}) - \beta^2(1 + \frac{\epsilon_i}{\epsilon_{max}}) - \delta\right] \tag{14}$$

from which one determines $\epsilon_{min}$ [12]. The $\epsilon_{min}$ here are of order $\epsilon_i/10$, with a weak $A$-dependence, which physically appears more reasonable.

In summary, there are two energy loss regimes in this model: (i) $\epsilon_{min} < \epsilon < \epsilon_i$ where the energy loss law is given by eq.(10). The entire atom is assumed to recoil which has negligible energy associated with it. Angular deflection of the muons associated with these events is considered as part of the multiple scattering off nuclei. (ii) $\epsilon > \epsilon_i$ where the basic loss law is eq.(6) and two body $\mu e^-$ kinematics is assumed. Angular deflection is correlated with energy loss. In the simulations this region is further divided into $(\epsilon_i < \epsilon < \epsilon_c)$, treated collectively, and $(\epsilon_c < \epsilon < \epsilon_{max})$ treated as individual events.

### 3.2 Angular Distribution

The angular distribution of a charged particle-nucleus encounter, stated per unit length in terms of *projected* angle, $\theta_x$, is assumed to be [9, 13]

$$v(\theta_x) = \frac{\pi}{2}\frac{N_{Av}}{A}\left(\frac{2Ze^2}{p\beta}\right)^2 \frac{1}{(\theta_x^2+\theta_0^2)^{\frac{3}{2}}} = \frac{K}{(\theta_x^2+\theta_0^2)^{\frac{3}{2}}} \tag{15}$$

where $p$ is the muon momentum, $e$ is the electron charge, and $\theta_0$ is an angle associated with screening of the nuclear charge by atomic electrons. Finite nuclear size and limited binding energy of the constituent nucleons suppress large angle scattering. This is modeled by applying a nuclear form factor to eq.(15).

The angles associated with electron encounters in the low energy transfer region $(\epsilon < \epsilon_i)$ are included in the nuclear scattering. The standard treatment includes the electrons by replacing $Z^2$ by $Z(Z+1)$ in eq.(15). Since the $\epsilon < \epsilon_i$ regime is only part ot the total $\mu e$ cross section, $Z^2$ is replaced here by $Z(Z+k)$ where $k = \sigma(\epsilon < \epsilon_i)/\sigma_{tot} < 1$. Put differently, the regime $\epsilon > \epsilon_i$, which is treated separately, must be excluded to avoid double counting. In most cases here $k$ will actually be very close to unity. For both nuclear and low energy transfer electron scattering a restriction threshold, $\theta_c$, is introduced for reasons entirely similar to those motivating $\epsilon_c$, viz., to provide a better approximation below $\theta_c$ at the expense of treating some events with $\theta > \theta_c$ individually.

For the regime $\epsilon_i < \epsilon < \epsilon_c$, which assumes free $\mu e$ scattering, the 4-momentum transfer to the muon equals that to the target electron:

$$q^2 = -2m_eT_e = (E_0 - E)^2 - (\vec{p_0} - \vec{p})^2 \simeq \frac{-m_\mu^2 T_e^2}{p_0^2} - p_0^2\theta_\mu^2 \tag{16}$$

where $T_e$ is the kinetic energy acquired by the electron, which—in two body kinematics—equals the muon's energy loss, and $\theta_\mu$ is the (polar) angle of the muon. The quadratic term in $T_e$ in the last part of eq.(16) may be neglected: only when $T_e$ approaches $\epsilon_{max} \simeq 2m_e p_0^2/m_\mu^2$ does it become comparable to $2m_e T_e$ but this concerns, only a small portion of all events and the restriction threshold, $\epsilon_c$, is typically set well below $\epsilon_{max}$. Summing over all collisions in a target

$$\sum \theta_\mu^2 = \frac{2m_e \sum T_e}{p_0^2 - 2E_0 \sum T_e} \tag{17}$$

where $\sum T_e$ corresponds to the total energy loss (obtained—collectively for many events—via the Edgeworth approximation). The denominator of eq.(17) approximates the average of $p^2$ when a $\mu$ starts at $p_0$ and loses $\sum T_e$ in energy. Eq.(17) is assumed to specify a Gaussian in projected angle with $\sigma^2 = \sum \theta_\mu^2/2$. The Gaussian assumption is somewhat questionable, especially if $\epsilon_c$ is set high. Since $\mu e$ scattering is assumed free in this regime there is a minimum angle, associated with the minimum energy transfer $\epsilon_i$, for each event: $\theta_\mu = \sqrt{2m_e\epsilon_i}/p$. This is of order of—but slightly larger than—the screening angle for nuclear scattering. This may help to establish the validity of the model at energy transfers near $\epsilon_i$, where the assumption of free $\mu e$ scattering becomes doubtful, since some screening applies to scattering off electrons as well.

Events with $\epsilon_c < \epsilon < \epsilon_{max}$ are simulated individually using eq.(6) directly to find $\epsilon$ and two-body kinematics to determine the angle. Since both $\mu$ end $e^-$ are assumed point-like, the maximum energy transfer follows entirely from kinematics. Because of the light electron mass individual angles are relatively small.

### 3.3 Restriction Thresholds

Choosing the restriction thresholds, $\epsilon_c$ and $\theta_c$, involves a compromise between how many events need to be simulated individually (as few as possible: high threshold) and how well the Edgeworth approximation holds (better at low threshold).

The choice is most important for energy loss where the Gaussian distribution is known to be less reliable. When $\epsilon_c \ll \epsilon_{max}$ the number of collisions above $\epsilon_c$ is roughly

$$n_> = \xi t \int_{\epsilon_c}^{\epsilon_{max}} \epsilon^{-2}\, d\epsilon \simeq \xi t/\epsilon_c \tag{18}$$

or $\epsilon_c \simeq \xi t/n_>$. For fixed $n_>$ note that $\epsilon_c \propto t$. For the Gaussian approximation to hold $\epsilon_c$ should preferably be less than $\sigma$ so that the Gaussian dominates the single scattering. For $\epsilon_c \ll \epsilon_{max}$, this means

$$\sigma^2 = t \int_0^{\epsilon_c} \epsilon^2 \omega(\epsilon)\, d\epsilon \simeq \xi t \epsilon_c. \tag{19}$$

Setting $\sigma = \epsilon_c$ in eq.(19) gives $\epsilon_c = \xi t$ which corresponds to eq.(18) with $n_> = 1$. Therefore, at this very approximate level, the $\epsilon_c$ for which the Gaussian holds is the same as the $\epsilon_c$ chosen such that only a few individual simulations are required. As will be seen in sec. 5, even for quite small $\epsilon_c$ the Gaussian fit is very approximate indeed and the Edgeworth series to higher order is needed to correct major discrepancies. As a practical matter one chooses $\epsilon_c$ as a fraction of $\xi t$ and, with $\epsilon_c \simeq \xi t/n_>$, one may equate the denominator roughly with the number of events above $\epsilon_c$.

For the angular distributions, the average number of individual events, in a target of thickness $t$, is determined by integrating eq.(15) above $\theta_c$: $n_> \simeq Kt/(2\theta_c^2)$. In practical situations one defines $\theta_c$ as a fraction of $\sqrt{Kt}$—similar to what is done for $\epsilon_c$. The denominator is then also related to $n_>$. If $n_>$ is of order unity, then $\theta_c^2 \simeq Kt/2$ while $\sigma^2 \simeq Kt[\ln(2\theta_c/\theta_0) - 1]$, from eq.(15), will typically be considerably larger which is why the Gaussian works somewhat better for multiple scattering.

# 4 Monte Carlo Implementation

Monte Carlo implementation of the model is along familiar lines. Selection from an Edgeworth series can be done quite efficiently. Eq.(1) has negative as well positive terms. In some places, usually far out in the tails, it may well predict 'negative probabilities'. These do not pose a problem here. Eq.(1) may be rewritten as

$$F(x) = \sum c_i x^i e^{-\frac{x^2}{2}}, \tag{20}$$

i.e., a sum over distributions of $\chi^2$ type, by collecting same-order terms from among the Hermite polynomials. In eq.(20) $x$ represents a standardized variable: $x = (\Delta E - \overline{\Delta E})/\sigma_{\Delta E}$ or $x = \theta_x/\sigma_\theta$. Whether a given term in eq.(20) is positive or negative depends on the signs of $c_i$, $x$, and on whether $i$ is even or odd. The basic strategy is to select a random $x$ from the terms of eq.(20) which are positive. Negative terms are taken into account by the Monte Carlo rejection technique.

Energy loss selection below $\epsilon_c$, which is divided into two brackets ($\epsilon_{min} < \epsilon < \epsilon_i$ and $\epsilon_i < \epsilon < \epsilon_c$) as decribed in sec. 3.1, is treated collectively using

the Edgeworth series. It is first decided to choose from among positive or negative $x$. Next, a specific term is selected from among the positive ones (proportional to $P_i = \int_0^\infty c_i x^i \exp(-x^2/2)\, dx$) followed by selection of $x$ from that term in the usual manner (see, e.g, ref. [10]). This $x$ is accepted or rejected by testing a random number versus the ratio of eq.(1) to the sum of its positive terms. For individual event selection the (random) number of such events is first chosen from a Poisson distribution characterized by the expected number of events. An energy ($\epsilon_c < \epsilon < \epsilon_{max}$), as per eq.(6), is then selected from an $\epsilon^{-2}$ distribution with the square bracket taken into account by rejection.

Angle selection below the cut-off $\theta_c$—for combined scattering off nuclei and off atomic electrons at low energy transfer—is also from an Edgeworth series and proceeds similarly to energy loss. However, since positive and negative $x$ have the same distribution, one selects $|x|$ first, then chooses its sign with equal probability. For angle selection associated with energy transfers $\epsilon_i < \epsilon < \epsilon_c$ off electrons, the mean square angle of the distribution $\sum \theta_\mu^2$ is determined following selection of an energy loss as per eq.(17). Random $\theta_x$ and $\theta_y$ are then chosen from a Gaussian with zero mean and $\sigma = \sqrt{\sum \theta_\mu^2/2}$. For individual selection the number of events is again assigned from a Poisson distribution. For each event (if any) a $\theta_x$ ($> \theta_c$) is chosen from a probability distribution proportional to eq.(15). After choosing a $\theta_x$ and $\theta_y$ the momentum transfer is tested for rejection versus a nuclear form factor as in [2].

# 5 Results

A few results are shown here by way of illustration, including some instances where the approximations described in this note can be checked directly versus exact results. One such possibility is to compare the restricted Vavilov ($J = 1/2$) distribution [2] with various orders of the Edgeworth expansion. The physical model used for this comparison is not the one from sec. 3 but one consistent with Vavilov's (implicit) assumption that Bhabha's formula holds down to some low energy, see eq.(9). The comparison is made here for 0.2 GeV muons incident on a beryllium target, 1 $g/cm^2$ thick. Maximum energy transfer in a single $\mu e$ collision is 3.59 MeV but a restriction threshold at $\epsilon_c = \xi t/2$ =43.6 keV is adopted. This means that on average 1.89 $\mu e$ collisions are left to be treated as individual events. Incidentally, the low energy limit, from eq.(9), is only about 0.006 eV in this case—much lower than can be physically justified.

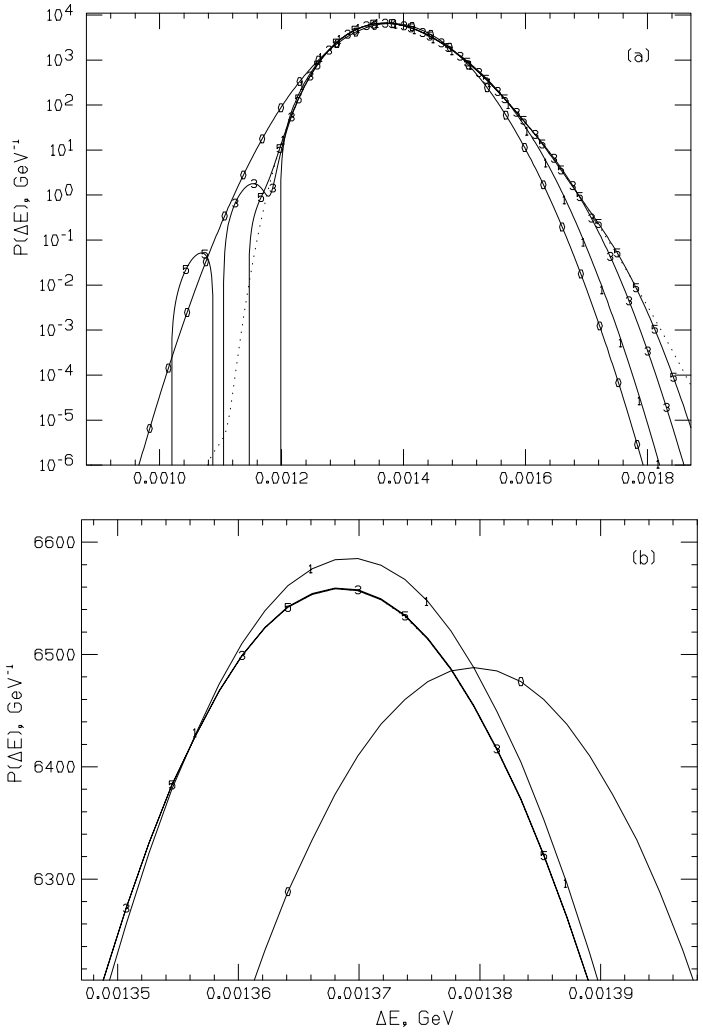


Figure 1: Restricted ($\epsilon < 43.6\ keV$) Vavilov distribution (dotted line) and various orders of Edgeworth expansion (solid lines), including 0th order (Gaussian) for 0.2 GeV muons on 1 $g/cm^2$ beryllium target. (a) Overall comparison over $\pm 8\sigma$, (b) detail of peak region (Vavilov curve coincides with 3rd and 5th order results in this graph).

Fig. 1a shows the Vavilov distribution along with the 0th (Gaussian), 1st, 3rd, and 5th orders of the Edgeworth expansion (2nd and 4th orders mostly interpolate their neighbors and are omitted merely for clarity of the

plot). The ordinate ranges over $\pm 8\sigma$ of the distribution. As can be seen the highest order matches quite well to analytic result except at very low $\Delta E$—although at that point one is several orders of magnitude below the peak. It can be seen that the Gaussian badly overestimates at low $\Delta E$ and underestimates at the high end. The same situation is depicted in fig. 1b but with only the peak region shown. The higher orders here completely cover the Vavilov curve while the discrepancy between them and the Gaussian is clearly exhibited. The same comparison is repeated in figs. 2a and 2b but with lower restriction threshold of $\epsilon_c = \xi t/10$ =8.72 keV at which point about 10 collisions must be treated indiviually. As can be seen the Gaussian is still not very accurate. Figs. 3a and 3b again represent the same case but at a larger threshold of $\epsilon_c = 2.5\xi t$ =218 keV above which about 0.32 collisions are expected to take place in the target. It can be seen that the algorithm has deteriorated although it is much preferable over a Gaussian. In fig. 4 shows how the energy loss Monte Carlo selection algorithm performs when $10^7$ muons strike the same beryllium target as for the case presented in fig. 1. Perhaps the unphysical hump at low $\Delta E$ can be discriminated against by comparing the sign of $\mathrm{P}(\Delta E)$ for successive orders of approximation. This requires some care but, since for each selection $\mathrm{P}(\Delta E)$ must be evaluated anyway, would not add significantly to computation time. It is also possible that using *incomplete* orders in eq.(1) may suppress the hump though most likely not without compromise elewhere. In most applications the hump will make little difference: in fig. 4 it accounts for 11 out of the $10^7$ events.

In sec. 3.1 an $\epsilon^{-3}$ energy dependence is assumed for energy losses below the average ionization potential, $\epsilon_i$, instead of the approximate $\epsilon^{-2}$ dependence of eq.(6). This distinction is important only for low restriction threshold, $\epsilon_c$, i.e., when it becomes of the same order of magnitudes as $\epsilon_i$ or, since $\epsilon_c$ is taken proportional to target thickness, for very thin targets. Fig. 5 pictures the case of 0.2 GeV/c muons incident on a 0.003 $g/cm^2$ thick beryllium target which places $\epsilon_c$ at 131 eV—or about twice the $\epsilon_i$ of 64 eV. The model of sec. 3.1 produces a broader and more Gaussian like distribution compared with the case where $\epsilon^{-2}$ holds troughout.

Since analytically derived *restricted* angular distributions are not readily available, comparison with the approximations offered here is more roundabout. For the case of 0.3 GeV/c muons on a 1 g/cm$^2$ beryllium target, fig. 6 compares the Molière distribution [14], using Bethe's formulation [15], with Monte Carlo output of the model of sec. 3 for $10^7$ muons. The Monte Carlo combines the Edgeworth series below $\theta_c = \sqrt{K}$ =0.0112 radians, with individual simulation above it (on average about 0.5 events). The Edgeworth approximation is carried out to 10th order which requires about the

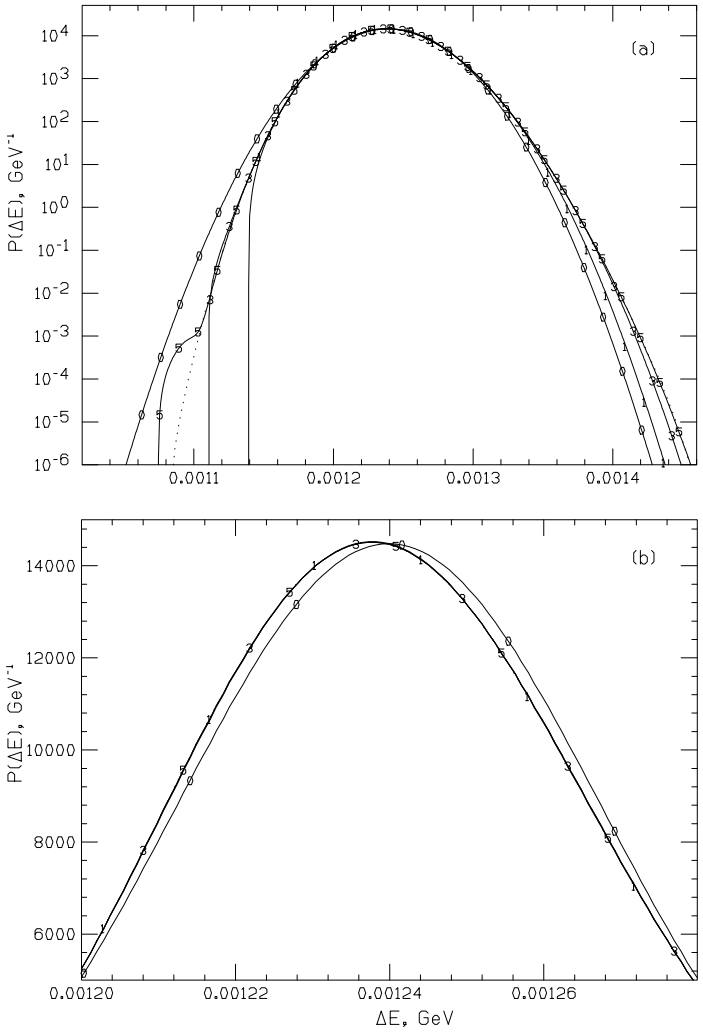


Figure 2: Restricted ($\epsilon < 8.76\ keV$) Vavilov distribution (dotted line) and various orders of Edgeworth expansion (solid lines), including 0th order (Gaussian) for 0.2 GeV muons on 1 $g/cm^2$ beryllium target. (a) Overall comparison over $\pm 8\sigma$, (b) detail of peak region (Vavilov curve coincides with 3rd and 5th order results in this graph).

same amount of computation as a 5th order energy loss calculation, thanks to vanishing of the odd cumulants. The same screening angle is used for the Edgworth series as for the Molière distribution. However, the precise form of

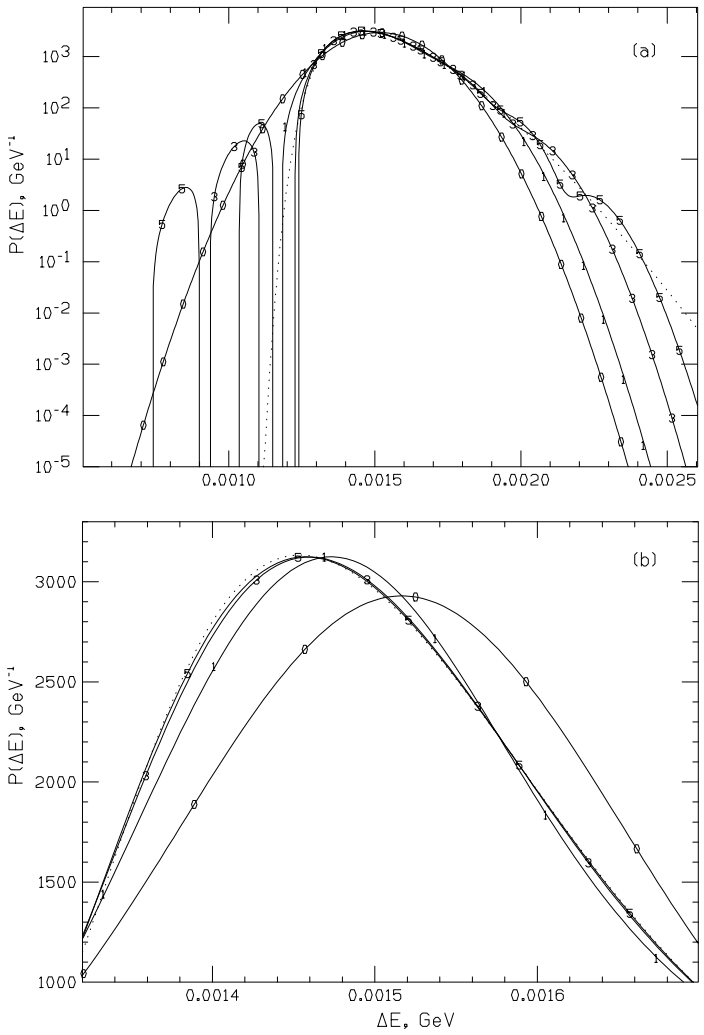


Figure 3: Restricted ($\epsilon < 218\ keV$) Vavilov distribution (dotted line) and various orders of Edgeworth expansion, including 0th order (Gaussian) for 0.2 GeV muons on 1 $g/cm^2$ beryllium target (solid lines). (a) Overall comparison over $\pm 8\sigma$, (b) detail of peak region.

the single scattering distribution, eq.(15), in the Edgeworth series does not correspond exactly to what is implicit in the Molière theory. Agreement is good overall and some small discrepancies (at the level of a few percent and invisible at the scale of fig. 6) are likely due to this lack of correspondence.

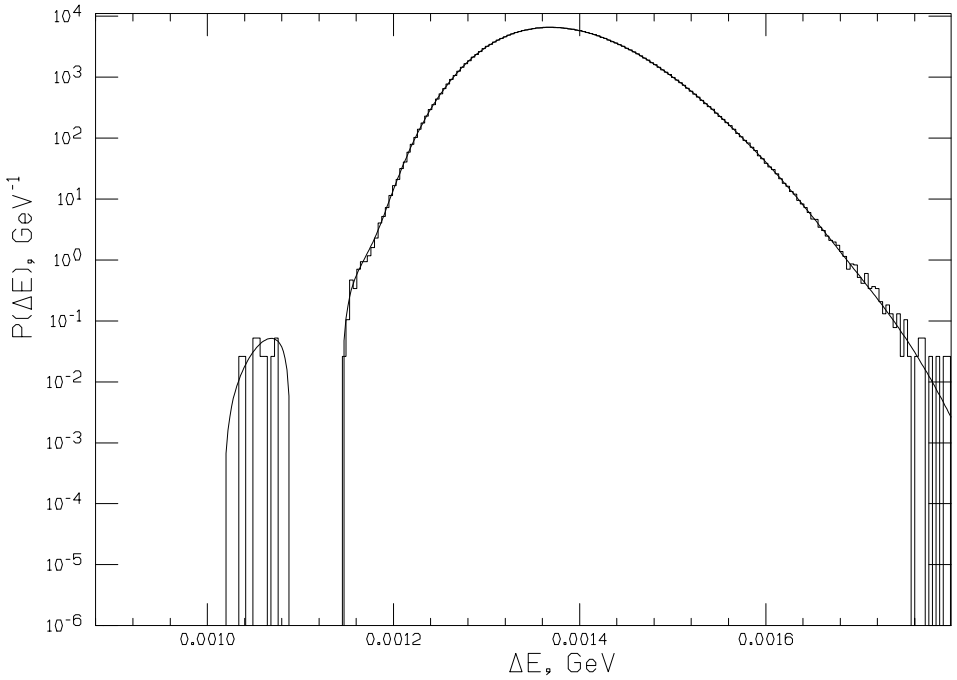


Figure 4: Histogram generated by Monte Carlo selection routine for $10^7$ muons on beryllium target (same case as fig. 1) *vs* directly calculated 5th order Edgeworth expansion.

Fig. 7 shows scatter plots of the correlations between energy loss and angle for $10^4$ muons of 0.2 GeV/c incident on 1 $g/cm^2$ of (liquid) hydrogen—for which correlations are likely to be most important. Separate plots are given for $\mu e$ Bhabha scattering which is individually simulated for an average of 1.79 events above $\epsilon_c (= \xi t/2)$ of 97.4 keV . Careful scrutiny reveals a line traversing the scatter plot which is comprised of those points corresponding to single event selection from the Poisson distribution. This line starts at $\Delta E = \epsilon_c$ while the diffuse scatter starts—as expected—at $\Delta E = 2\epsilon_c$, since at least two events are needed to produce a spread in angle at a given $\Delta E$. Strong energy angle correlations remain even with multiple events although the angles are quite small due to kinematics. Also shown is the correlation for $\mu e$ scattering in the energy loss regime $\epsilon_i < \epsilon < \epsilon_c$ which is much smaller because one sums over many events after which the only effective correlation which remains is between energy loss and the variance of a Gaussian. The final plot of fig. 7 shows the correlations when all processes are included.

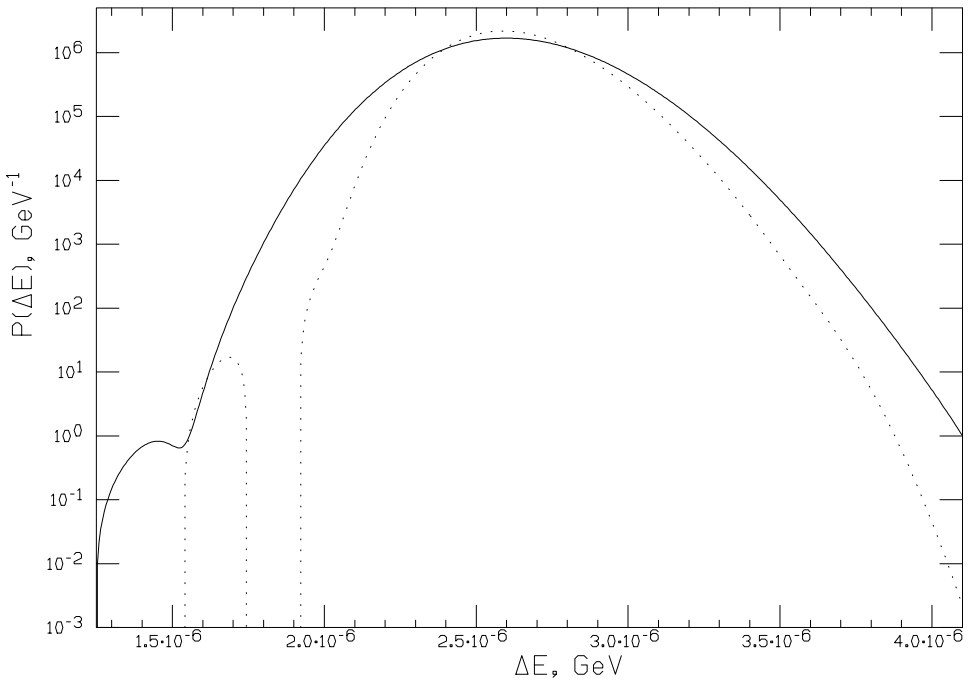


Figure 5: Fifth order Edgeworth series for the model of sec. 3 (solid line) as well as for the Vavilov distribution (dotted line) for 0.2 GeV/c muons incident on $0.003 g/cm^2$ beryllium target with restriction threshold at 131 eV. Effect is much less for thick targets.

In this last case the correlation coefficient, $< \Delta E \theta > / \sigma_{\Delta E} \sigma_\theta$, equals 0.038 which is perhaps not entirely negligible in ionization cooling. It is higher for thinner targets, e.g., if the thickness in the present example is reduced to 0.05 $g/cm^2$ the correlation coefficient increases to 0.10.

# 6 Concluding Remarks

The Edgeworth expansion can play a useful role in describing distributions of energy loss and multiple scattering angle. It builds on the (two parameter) Gaussian by inclusion of the higher moments of the single event distribution as parameters to generate successively better approximations. To sufficiently high order, it can replicate quite well both the Vavilov distribution of energy loss and the Molière distribution of multiple scattering. Monte Carlo

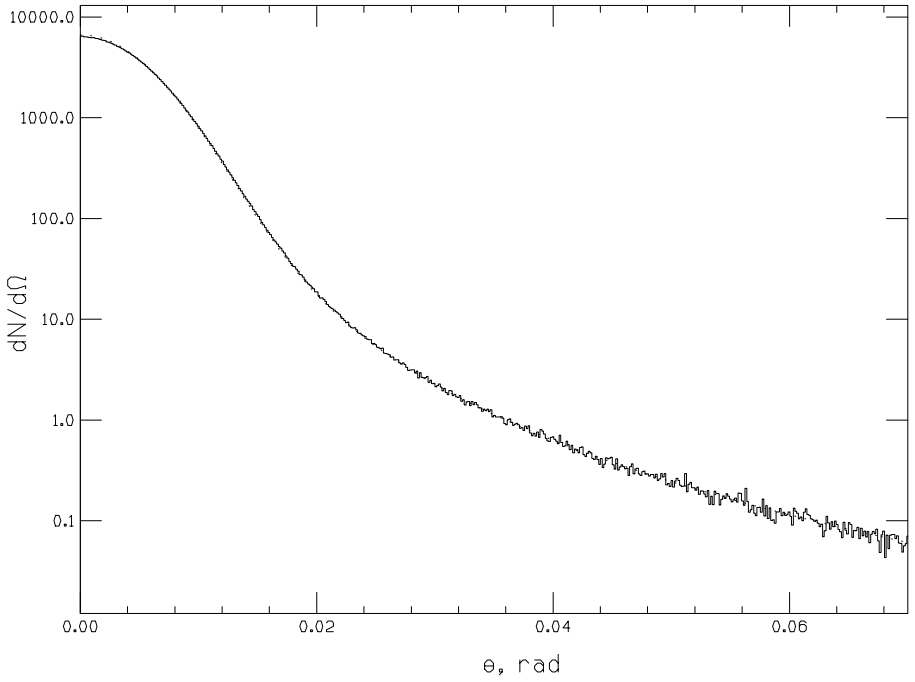


Figure 6: Molière distribution (dotted line) compared with simulation of 10th order Edgeworth series plus individual events above 0.0112 radians for $10^7$ muons of 0.3 GeV/c on 1 $g/cm^2$ beryllium target (histogram).

selection algorithms based on the expansion are relatively easy to encode and efficient in their execution. The Edgeworth expansion is especially appealing for simulations since it allows ready translation from physical model (via the moments of the single event distribution) to selection algorithm. It offers flexibility: order of expansion, step size, and restriction threshold may all be tailored to a specific application or might be made adjustable within the calculation for optimum performance. Details of implementing this will depend heavily on the required accuracy and available computing resources.

Use of the Edgeworth expansion in the present applications is motivated by its relation to the Gaussian—already well known to be a good approximation for energy loss and projected angle distribution in thick targets. Future investigations may explore expansions using other orthogonal polynomials. These may work better for very thin targets or high restriction thresholds. The physical model presented here obviously needs more work to improve some of the oversimplifications. In particular treating atomic

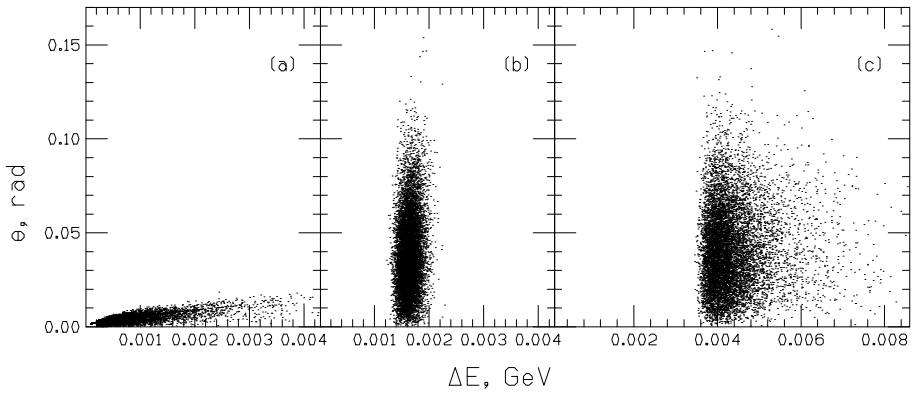


Figure 7: Scatter plots generated with model of sec. 3 to illustrate energy loss *vs* angle correlations for 0.2 GeV/c muons incident on 1 $g/cm^2$ of liquid hydrogen (a) for individually simulated Bhabha scattering, (b) for $\epsilon_i < \epsilon < \epsilon_c$ regime and (c) all processes combined.

electrons as free for modest energy transfers as well as the sharp demarcation between bound and free at the mean ionization potential may need further refinement. For more precise work a general model may not suffice and one would concentrate instead on the detailed atomic structure of each material of interest. The Edgeworth series will still be able to provide good approximations to the energy loss and angular distributions based on such detailed models.

The entire approach may succeed in other applications as well—given the ease with which it carries over from energy loss to multiple scattering. Thus, whenever a distribution satisfies a general transport equation, as typified by eqs.(2) and (7), the same type formulae for the $\kappa_i$ result and eq.(1) provides a successively improving approximation which is well suited for Monte Carlo sampling. Taking advantage of restriction thresholds can greatly improve the accuracy of the simulation.

My thanks to N. Mokhov for comments and discussion and to D. Neuffer for a careful reading of the manuscript.

# References

[1] see, e.g., C. Ankenbrandt et al., Fermilab-Pub-98/179 (1998).

[2] A. Van Ginneken, Nucl. Inst. Meth. **A362**, 213 (1995).

[3] N. V. Mokhov and S. I. Striganov, Proc. 9th Advanced IFCA Beam Dynamics Workshop, p. 234, Montauk, N.Y., 1995.

[4] H. Cramér, *Mathematical Methods of Statistics*, Princeton Univ. Press (1945).

[5] This is true on general grounds but has not been investigated for this particular application.

[6] L. Landau, J. Phys. (Moscow) **8**, 201 (1944).

[7] P. V. Vavilov, Zh. Eksp. Teor. Fiz. **32**, 920 (1957); Sov. Phys. JETP **5**, 749 (1957).

[8] H. J. Bhabha, Proc. Roy. Soc. London **164**, 257 (1938).

[9] J. D. Jackson, *Classical Electrodynamics*, 2nd Ed., Wiley, New York (1975).

[10] C. Caso et al., Eur. Phys. J. C **3**, 1 (1998).

[11] R. M. Sternheimer, M. J. Berger and S. M. Seltzer, At. Data and Nucl. Data Tables, **30**, 261 (1984).

[12] The last term in the bracket of eq.(12) appears to belong in the $dE/dx$ formula. Perhaps it is neglected in the usual presentations because it is typically very small (especially for $dE_{restr}/dx$) and by dropping it one avoids introducing projectile spin dependence. Here it is assumed to be present in eq.(12) and then subtracted out in arriving at eq.(14).

[13] $v(\theta_x)$ expresses essentially the same scattering law as $\omega(\epsilon)$ since $\theta(= \sqrt{\theta_x^2 + \theta_y^2})$ and $\epsilon$ are uniquely related via two body kinematics. However, eq.(6) is the full cross section for $\mu e$ scattering whereas eq.(15) represents an approximation to it—which is further modified by the screening angle $\theta_0$ to adapt to nuclear scattering. When referring to angular distributions eq.(15) is the Rutherford approximation. When translated to an energy loss distribution it corresponds to the Landau approximation.

[14] G. Molière, Z. Naturforsch. **3a**, 78 (1948).

[15] H. Bethe, Phys. Rev., **98**, 1256 (1953).